Regular Article

PHYSICAL CHEMISTRY RESEARCH
Published by the
Iranian Chemical Society
www.physchemres.org
info@physchemres.org

***Phys. Chem. Res.**, Vol. 5, No. 2, 239-251, June 2017*
DOI: 10.22036/pcr.2017.40717

Theoretical Study on the Chemical Reactivity in the Armchair Single-walled Carbon Nanotube: Proton and Methyl Group Transfer

B. Achouri[a,b], Y. Belmiloud[a] and M. Brahimi[a,*]

[a]*Laboratoire de Physico Chimie Théorique et Chimie Informatique. Faculté de Chimie. Université des Sciences et de la Technologie Houari Boumediene (USTHB). BP N° 32 El Alia. Alger. Algérie.*

[b]*Centre de Recherches en Analyses Physico Chimiques. (CRAPC). Alger, Algérie.*

(Received 19 September 2016, Accepted 28 November 2016)

Proton transfer (PT) and methyl group transfer (MGT) occurring in small biomimetic systems, Formamide-Formamidic acid (FA-FI), and N-formyl-N-methylformamide-(E)-methyl N-formylformimidate (NMFA-NMFI) are investigated in the gas phase and in single-walled carbon nanotubes by using the density functional theory and the ONIOM approach. It is shown that PT reaction is disfavoured in single-walled CNT (5,5) because it increases the energy barrier, while confinement in CNT (6,6) decreases the energy barrier of MGT.

Keywords: Carbon nanotube, Proton transfer, Methyl group transfer, ONIOM and DFT

INTRODUCTION

Carbon nanotubes (CNTs), prepared experimentally in 1991 [1], have applications in several fields because of their optical, electronic, and mechanical properties, including their potential biocompatibility in pharmaceutical research for creating polyvalent drug delivery systems [2-8].

The nanotechnology approach based on drug administration control, has played a key role, particularly for the targeted delivery of drugs for several diseases such as tuberculosis, malaria, cancer and AIDS [9-16].

CNTs are, in fact, listed among the most powerful drug carriers because of their non-reactivity with transport drugs and also biocompatibility.

CNTs have been functionalized to increase their solubility in blood, and then they have been used as efficient delivery systems, especially for carboplatin [16-19]. The therapeutic agent and some ferromagnetic materials are placed inside. Hilder and Hill modelled the acceptance condition for the anti-cancer drug cisplatin inside a CNT based on the CNT diameter [20,21].

*Corresponding author. E-mail: mez_brahimi@yahoo.fr

Single-walled carbon nanotubes (SWCNTs) are new molecular-scale wires with useful properties for various potential applications, which include miniature biological devices [22].

We consider the possibility that proton transfer (PT) and methyl group transfer (MGT) occur inside the SWNTs with different diameters. We have investigated, with the help of theoretical methods, small-sized molecular models presenting such transfers. The examples illustrated here compare the effects of confinement on the molecules with their unconfined state (isolated state).

In biochemistry, PT, Proton Coupled Electron Transfer PCET [23-28] and MGT reactions are important processes and the mechanism of their enzymatic catalysis is of great interest. For example, the Formamide (FA)-Formamidic acid (FI) tautomerization (Fig. 1) has been used to model the tautomerization of DNA nucleobases-in particular, the tautomerization of guanine and uracil.

MGT reactions play an important role because they encompass homogeneous as well as heterogeneous catalysis and organic synthesis [29,30]. It has been specifically formulated to enhance the methylation pathways involved in homocysteine metabolism [31-34]. Several mechanisms

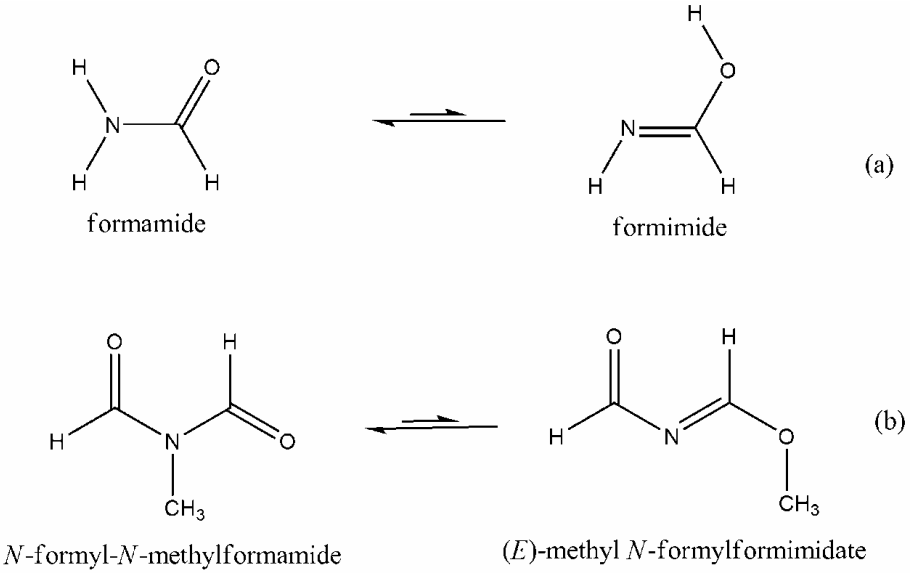

Fig. 1. The PT (a) and MGT (b) equilibrium.

have been proposed to describe MGT for DNA repair and other biological systems [35-38].

The aim of this work is to present a quantum chemical investigation of the confinement effects on the mechanisms of PT and MGT reactions in SWCNT. We applied the density functional theory (DFT) [39] to localize the stationary points for reactants, transition states (TSs), and products on the potential energy surface (PES). We considered small-sized molecular models in which PT and MGT can take place in steps or through a concerted mechanism [40]. We focus on the following reactions:

- FA which leads to FI, confined within armchair (5,5) SWNTs.
- NMFA which leads to NMFI, confined within armchair (5,5) and (6,6) SWNTs.

We have used the two layers of ONIOM calculations- this approach allows us to study the essential parts of the molecular systems at a higher level of theory, while the other less important part is studied at a computationally lower level [41], in order to explore the influence of the CNT confinement on PT and MGT reactions.

COMPUTATIONAL METHODS

The geometries of all structures in the gas phase were fully optimized by using the Gaussian 09 program package [42] at the DFT level, with the use of the hybrid functional B3LYP with the 6-31G (d) basis sets [43]. For the molecules confined in carbon nanotubes, full geometry optimizations were carried out with the two-layered ONIOM approach [41,44]. Vibrational frequency calculations have been carried out to determine the zero point energy (ZPE) corrections and the nature of the stationary points.

Small basis sets stabilize the complex more than the separate components because of the basis set superposition error (BSSE) [45,46]. The latter is due to the fact that the wave function of the monomer is expanded in much less basis function than the wave function of the complex. One solution for BSSE is the use of extremely large basis sets. This is, however, hardly feasible for most of the biochemically interesting systems. The second approach, employed in this work is the counterpoise method (CP) [47] which is an approximate method for estimating the size of the BSSE. The counterpoise interaction energy correction can, in most simple cases be calculated by:

$$E_{int} = E(AB, r_c)^{AB} - E(A, r_c)^{AB} - E(B, r_c)^{AB}$$

The notation AB indicates that the complexes, as the way

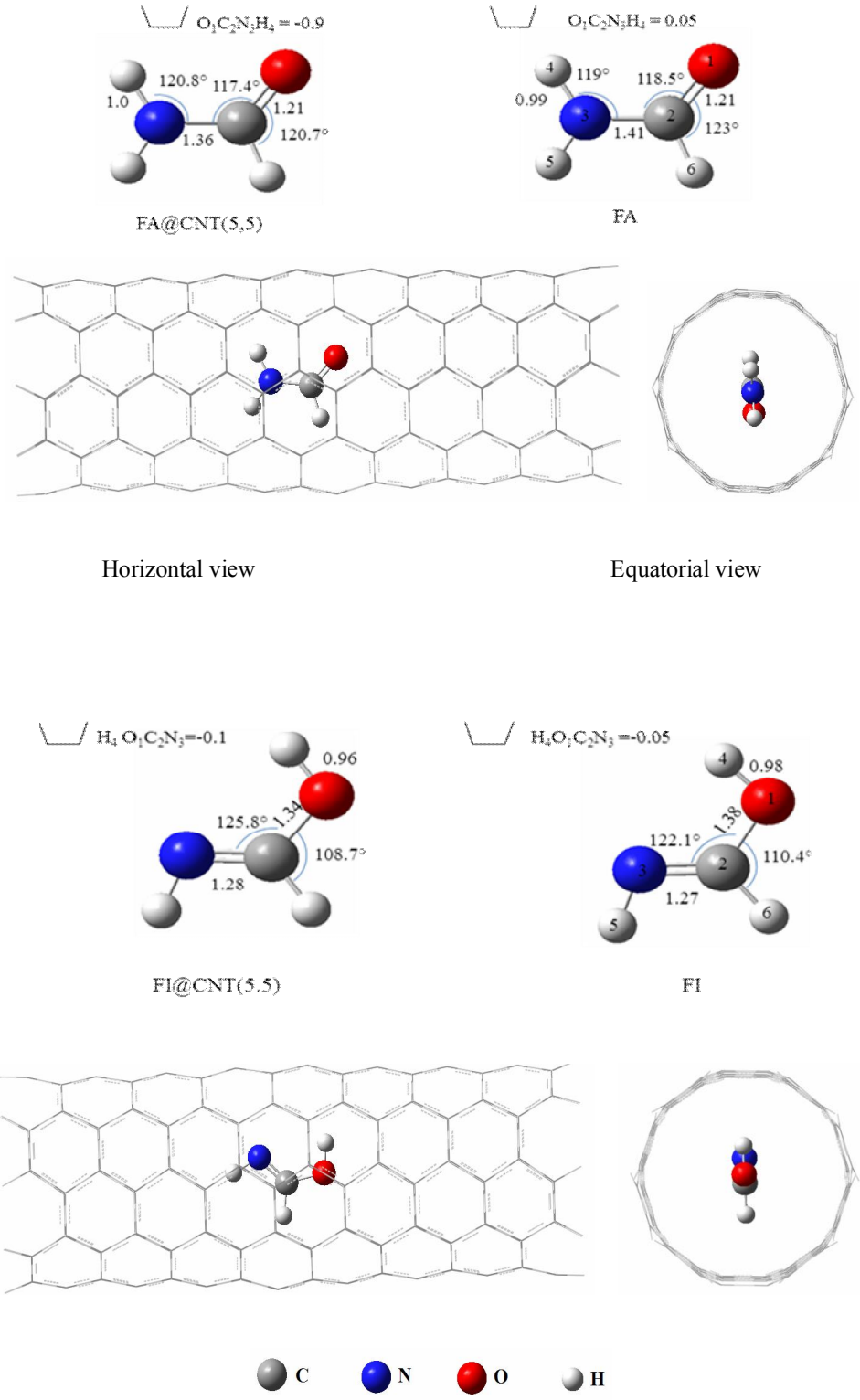

Fig. 2. FA and FI geometries isolated molecule and encapsulated molecule in CNT (5,5).

for the separate components, are calculated in the same absolute basis. The label r_c indicates the geometry of the product complex AB, while r_c indicates the geometry of the separate reactants.

To estimate solvation effect, the optimized geometries were carried out by the polarizable continuum model (IEF-PCM) [42-44] at the B3LYP/6-31G (d) level with different dielectric constants that correspond to dichloromethane (CH_2Cl_2, ε_r = 8.9) and tetrachloromethane (CCl_4, ε_r = 2.2) [40].

The CNT is placed into the lower layer and treated by the universal field force (UFF) [48]. It has been demonstrated that the combination of the density functional theory (DFT) and the UFF molecular mechanics is an appropriate method for modelling those reactions that do not lead to covalent interactions with SWCNT [49-51]. Each transition state (TS) exhibits one imaginary frequency. As for the armchair (5,5) and (6,6) SWCNTs, hydrogen atoms were added to saturate the valences of the ending carbons to avoid dangling bonds.

RESULTS AND DISCUSSION

Geometries of PT Reaction

Formamide tautomerization has been theoretically studied by Ai-ping Fu *et al.*, who employed the MP2 and B3LYP methods with different basis sets [52]. Here we will consider the PT reaction inside CNTs. The length of the molecular tube segment used consists of seven rows of benzenoid units, namely $C_{160}H_{20}$ for CNT (5,5). FA and FI structures in the isolated and confined CNTs are illustrated in Fig. 2, where bond lengths are in angstroms (Å) and bond angles are in degrees.

It can be seen that the C-N bond length in FA@CNT (5,5) diminishes by 0.05 Å compared with the isolated FA. The NCO and $O_1C_2H_6$ bond angles are narrowed to 117.4° and 120.7°, respectively. An increase of about 3.7° in the NCO angle is observed for the FI@CNT (5,5) molecule.

The geometrical parameters of the TS for the PT reaction are reported in Fig. 3. N-H and O-H distances in the TS are decreased to 1.33 and 1.30 Å, respectively by the confinement in CNT (5,5). The C-N bond length is shorter by 0.04 Å. The $O_1C_2H_6$ angle of TS@CNT (5,5) is decreased to about 13.8°. It is clear that the structure of the TS is slightly affected by the confinement of CNT (5,5).

Energetic of PT Reaction

We estimate the encapsulation energy by the following formula [53]:

$$E_{encaps} = E_{isome@CNT} - (E_{isomer} + E_{CNT})$$

The negative value of E_{encaps} indicates that the encapsulation is an exothermic process [54] (see Table 1).

Our calculated energy barrier for the isolated FA is 44.6 kcal.mol^{-1}, with the inclusion of ZPE corrections at the B3LYP/6-31G* level of theory. For FA@CNT (5,5), the TS is 51.4kcal.mol^{-1} above the energy of the equilibrium geometry (see Table 2). The activation energy of the PT reaction for the encapsulated FA is about 6.8 kcal mol^{-1} higher than the isolated one, suggesting that the PT reaction of FA may be controlled by the encapsulation within CNT (5,5). Figure 4 shows the relative energy of the PT reaction for both the isolated and confined systems. The energy difference between FI@CNT (5,5) and FA@CNT (5,5) is about 1.87 kcal mol^{-1} higher than the difference between the isolated FA and FI. These results are in line with the widely accepted view that CNT encapsulations can significantly affect the energies of chemical reactions [55].

Geometries of the Methyl Group Transfer Reaction

Large numbers of studies have shown that methyl transfer proceeds via a simple MGT transition state [56,57]. The intramolecular methyl transfer is found to proceed either through a methyl inversion mechanism or a methyl retention mechanism. In NMFA, only the methyl retention mechanism has been located.

We have first studied the insertion of NMFA and NMFI into CNT (5,5) and CNT (6,6). The computed encapsulation energies are reported in Table 3. The encapsulation of NMFA in CNT (5,5) is a highly endothermic process and thus we will not further consider this system. The geometrical parameters of the different isomers for the MGT isolated and encapsulated inside CNT (6,6) are reported in Figs. 5 and 6.

It can be seen that confined minimum energy geometries are somewhat different from those of the isolated system. The C_2-N_3, C_6-N_3 and C_4-N_3 bond lengths of the confined

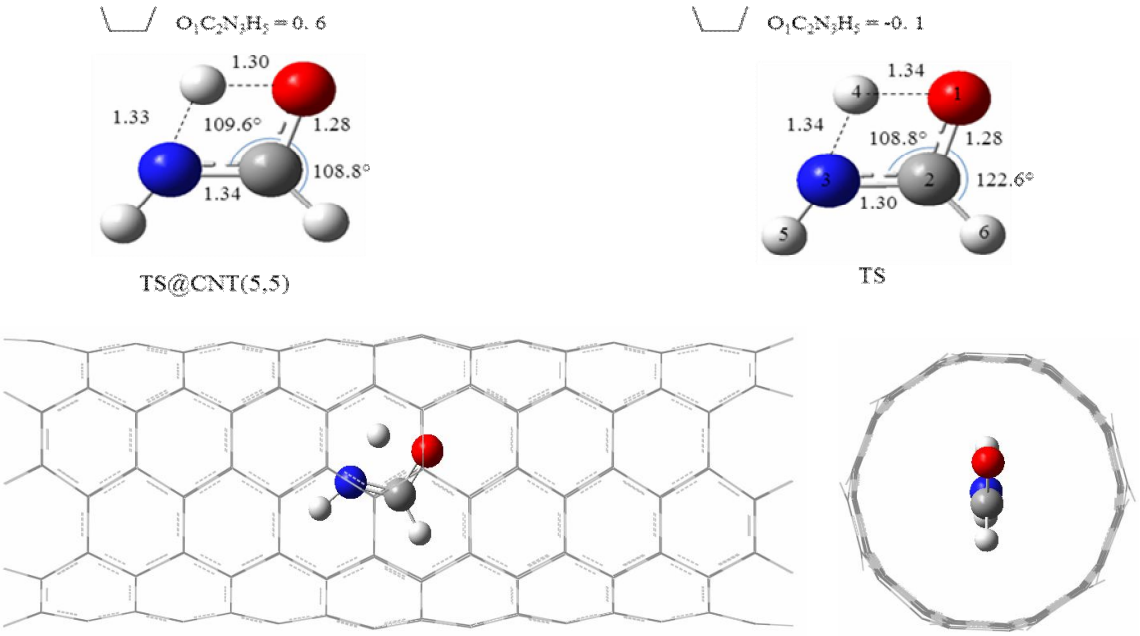

Fig. 3. Transition state for PT reaction in the isolated molecule and encapsulated molecule in CNT@ (5,5).

Table 1. Isomers, Encapsulation and BSSE Energies of PT Reaction Calculated at ONIOM (B3LYP/6-31G[a]: UFF) Level of Theory

	$E_{Isomer@CNT(6,6)}$ (a.u.)	E_{encaps} (Kcal mol^{-1})[a]	BSSE energy (Kcal mol^{-1})
FA	-167.394813	-50.67	6.82
FI	-167.368819	-48.34	6.85

[a]$E_{encaps} = E_{isome@CNT} - (E_{isomer} + E_{CNT})$; $E_{FA(isolate)} = -169.888843$; $E_{NMFA(isolate)} = -169.866563$ a.u. by B3LYP/6-31G*levels; $E_{CNT(5,5)} = 2.57478$ a.u. by UFF.

NMFA@ (6,6) are shorter than those of the isolated NMFA. In fact, they are shorter by 0.01, 0.02 and 0.03 Å, respectively. The $C_6N_3C_4$ bond angle is compressed from an equilibrium value of 5°, while the $C_2N_3C_6$ and $C_2N_3C_4$ bond angles are increased by about 4.4 and 0.7°, respectively.

The geometrical analysis of NMFI@CNT (6,6) does not show a big change in going from the isolated state to the confined one. The C_6-O_1 bond length is compressed by 0.01 Å. The bond angles of $C_2O_1C_6$ and $O_1C_2N_3$ are increased by 1.0 and 2.1°, respectively, while the $C_2N_3C_4$ angle is compressed by 4°.

The MGT transition state adopts two different forms TS1 (syn) and TS2 (anti) as confirmed by IRC calculations [40]. The TS1 is the lowest energy transition state leading to NMFI formation. Force constant calculations confirmed that TS1 has one imaginary frequency (see Table 4). The geometrical parameters of the two transition states of different complexes are presented in Fig. 5. No significant

Table 2. Relative Energies for the Isomers of PT Reaction

	Relative energy (Kcal mol^{-1})	Imaginary frequency (cm^{-1})
FA	0	
FI	13.60[a]	
TS	44.60[a]	-1937 cm^{-1}
FA@CNT (5,5)	0	
FI@CNT (5,5)	15.61[b]	
TS @CNT (5,5)	51.47[b]	-1936 cm^{-1}

[a]Relative energy calculated at B3LYP/6-31G* levels. [b]Relative energy calculated at ONIOM (B3LYP/6-31G*: UFF) levels.

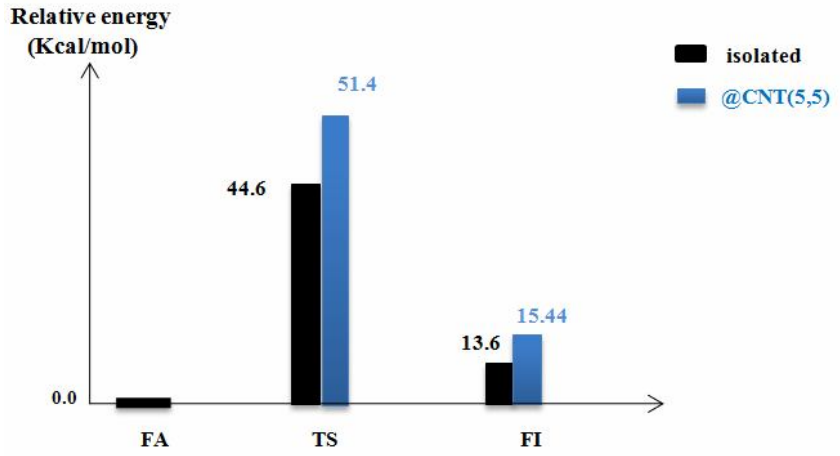

Fig. 4. A schematic view of the PT reaction in the isolate molecule and encapsulate molecule in CNT (5,5).

Table 3. Isomers, Encapsulation and BSSE Energies of MGT Reaction Calculated at ONIOM (B3LYP/6-31G*: UFF) Level of Theory

	$E_{Isomer@CNT(6,6)}$ (a.u.)	$E_{Isomer@CNT(5,5)}$ (a.u.)	E_{encaps} (Kcal mol^{-1})	BSSE energy (Kcal mol^{-1})
NMFA	-320.041918	-319.814718	90.40[a]	
			-17.79[b]	5.9
NMFI	-319.982077	-319.974636	-29.26[a]	
			0.5[b]	5.7

$E_{NMFA(isolate)}$ = -322.533566; $E_{NMFI(isolate)}$ = -322.502774 a.u. at B3LYP/6-31G* levels. [a]E_{encaps} in CNT(5,5); [b]E_{encaps} in CNT (6,6). $E_{CNT(5,5)}$ = 2.57478 a.u.; $E_{CNT(6,6)}$ = 2.52 a.u. at UFF levels.

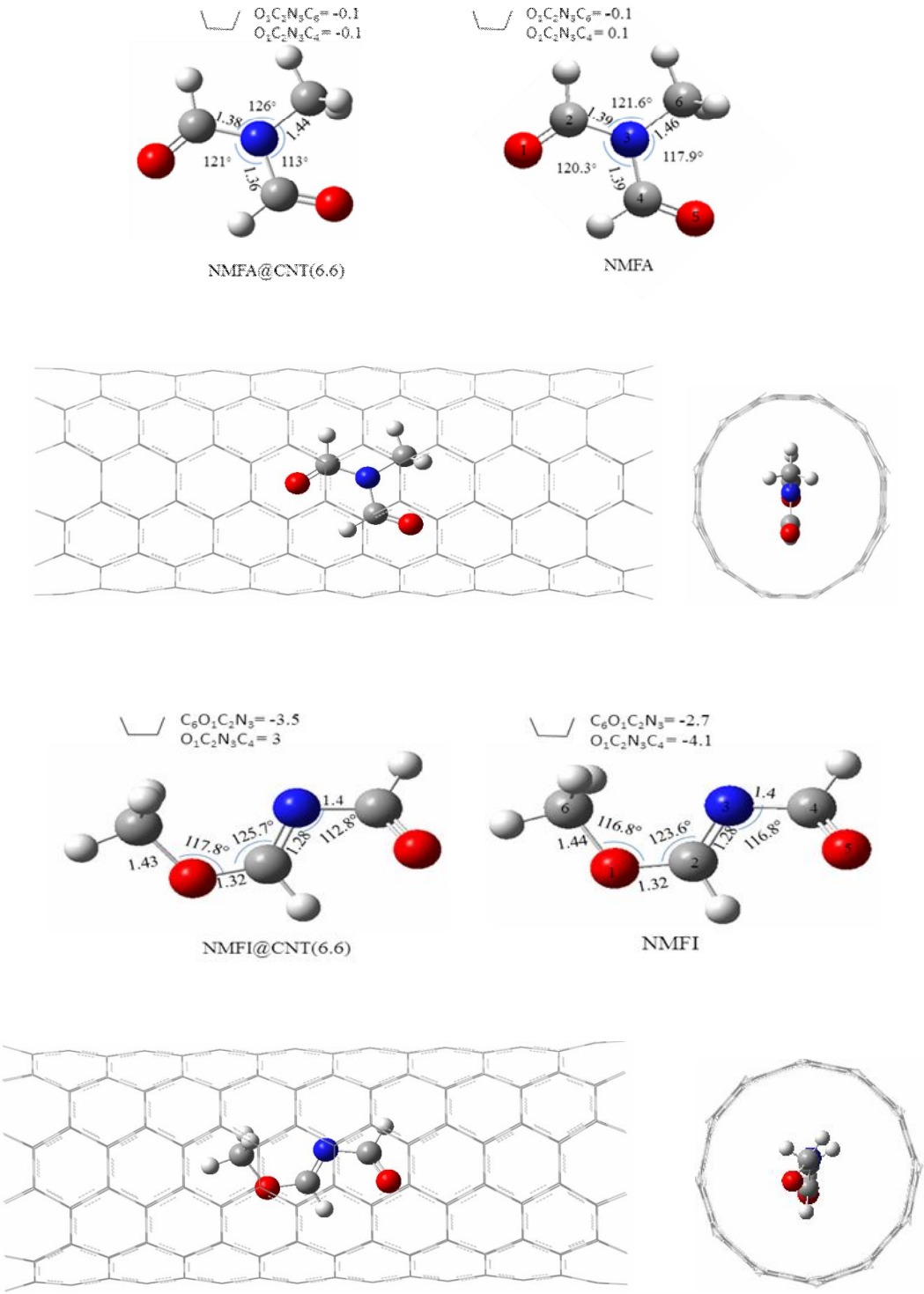

Fig. 5. The optimized structures of NMFA, NMFI in the isolated molecule and encapsulated molecule in CNT (6,6) systems.

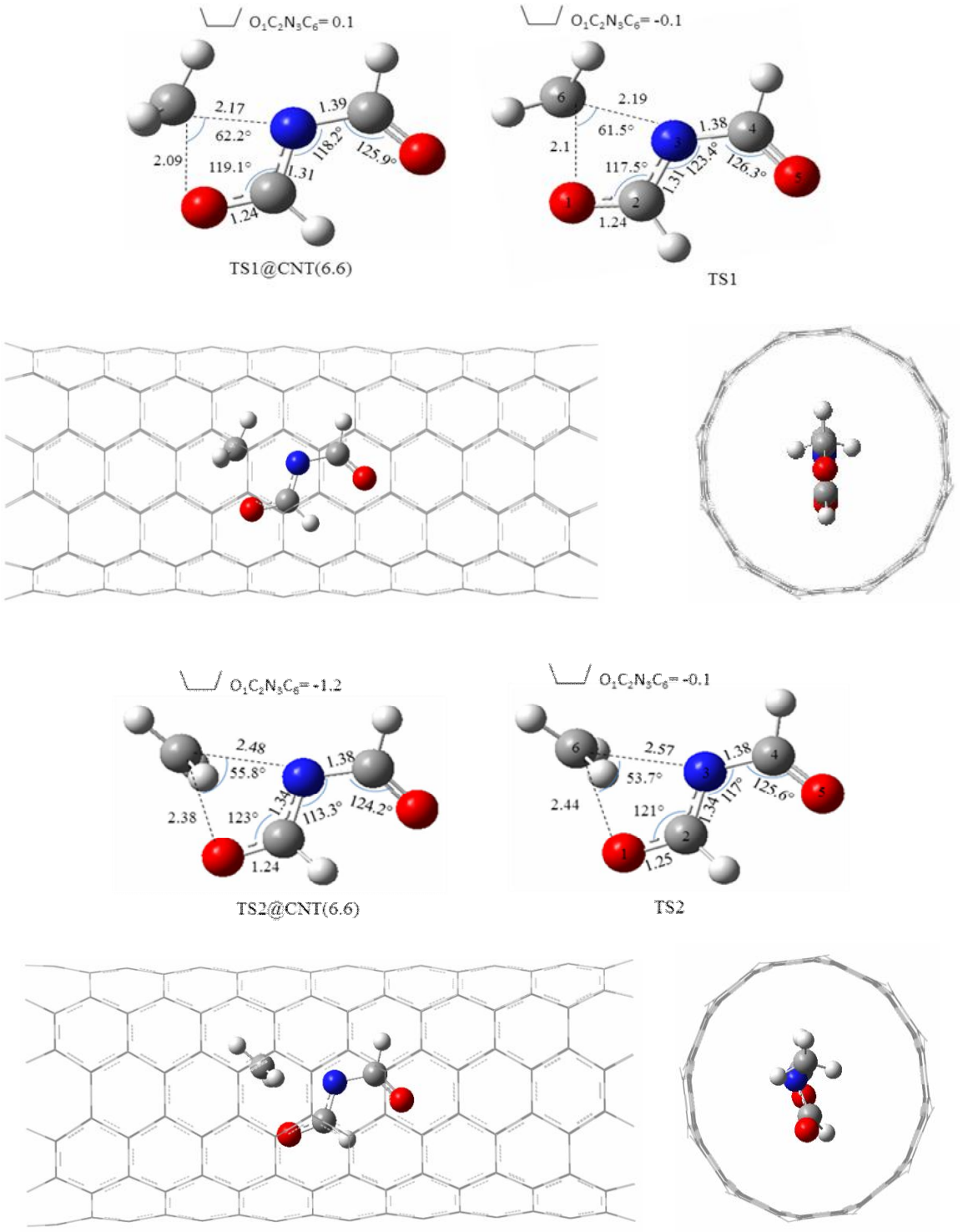

Fig. 6. Molecular structures of the transition states TS1 and TS2 for MGT reaction of the isolated molecule and encapsulated molecule in CNT@ (6,6).

Table 4. Relative Energies for the Isomers of MGT Reaction

	Relative energy (Kcal mol^{-1})	Imaginary frequency (cm^{-1})
NMFA	0	
NMFI	19.28[a]	
(TS 1)	67.96[a]	- 584.3003
(TS 2)	101.12[a]	- 685.2514
NMFA@CNT (6,6)	0	
NMFI@CNT (6,6)	34.52[b]	
(TS 1) @CNT (6,6)	63.0[b]	- 548.9849
(TS 2) @CNT (6,6)	94.53[b]	- 689.4142

[a]Relative energy at B3LYP/6-31G* levels. [b]Relative energy calculated at ONIOM (B3LYP/6-31G*: UFF) levels.

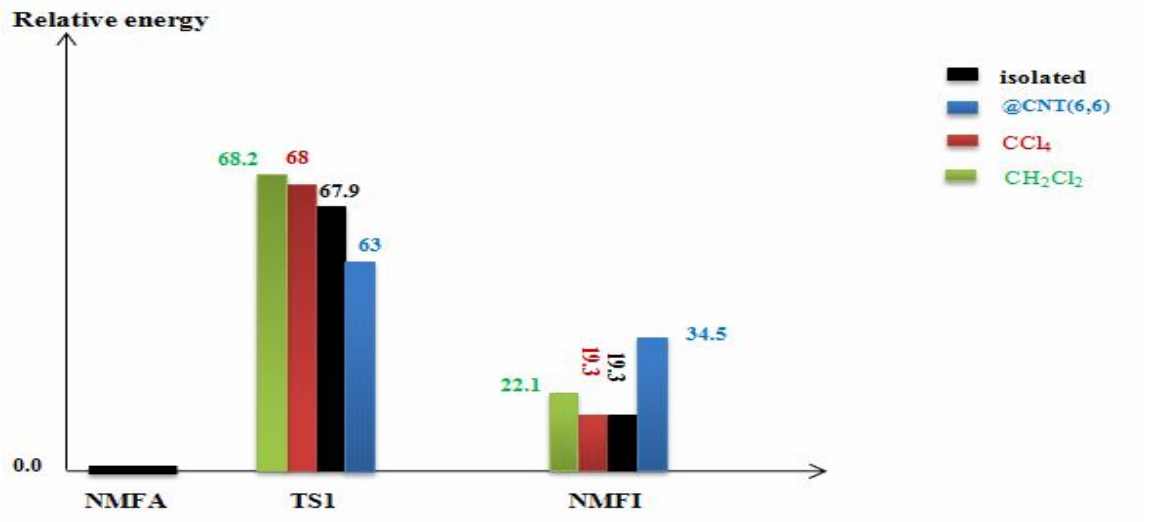

Fig. 7. A schematic view for energetic of MGT in the gas phase, in different solvents (CH_2Cl_2, CCl4) and in CNT (6,6).

change is observed in the structures of TS1 while passing from the isolated molecules to the confined CNT (6,6).

As an example of C_6-O_1 and C_6-N_3, the distances of the confined molecules are shorter by about 0.01 and 0.02 Å, respectively, than those of the isolated molecules; the $O_1C_6N_3$ and $O_1C_2N_3$ bond angles increased by about 0.7, 1.6 degrees, respectively; and the $C_2N_3C_4$ bond angle is compressed by 5.2°. The same also holds for TS2 the C_6-O_1 and C_6-N_3 distances of the confined molecules are shorter by about 0.06 and 0.1 Å, respectively. For the isolated

species, the $O_1C_6N_3$ and $O_1C_2N_3$ angles increase about 2.0 and 2.1°, respectively. The $C_2N_3C_4$ bond angle changes from 117° to 113.3°.

Energetic of the Methyl Group Transfer Reaction

The encapsulation of NMFA into CNT (6,6) and NMFI into CNT (5,5) are exothermic processes (Table 3**)**. The activation energy of TS1@CNT (6,6) is about 63kcal.mol^{-1} compared to the NMFA@CNT (6,6) energy (see Fig. 7). In comparison with the isolated state, the activation energy of the MGT reaction is lower by 4.9 Kcal mol^{-1} (TS1) with respect to TS1@CNT (6,6) while the energy barriers are lower by about 28.5 Kcal mol^{-1} with respect to NMFA@CNT (6,6). The encapsulation effects are significantly higher than the solvent effects. Our results have shown small changes in the energy barriers when the reaction occurs in CH_2Cl_2 and CCl_4 solvent [40].

The MGT reaction is notably affected by the confinement CNT (6,6) in view of geometries and energy. The confinement CNT (6,6) has an influence on the structures and energy barriers, and the activation energies obviously decrease slightly.

The most interesting result in this work is the important change for the internal energy variation of MGT reaction inside the CNT (6,6), which could mean that the regeneration of the DNA would be better in CNT.

In all our calculations, the BSSE is less than 7 Kcal mol^{-1} (See Tables 1 and 3), which could mean that it does not affect on the final results and related discussion.

REFERENCES

[1] Iijima, S., Helical microtubules of graphitic carbon. Nature. **1991**, 354, 56-58. DOI: 10.1038/ 354056a0.

[2] Akturk, A.; Goldsman, N.; Pennington, G.; Wickenden, A., Terahertz current oscillations in single-walled zigzag carbon nanotubes. *Phys. Rev. lett.* **2007**, *98*, 166803. DOI: 10.1103/ PhysRevLett.98.166803.

[3] Postma, H. W. C.; Teepen, T.; Yao, Z.; Grifoni, M.; Dekker, C., Carbon nanotube single-electron transistors at room temperature. *Science.* **2001**, *293*, 76-79. DOI: 10.1126/science.1061797.

[4] Tseng, Y. C.; Xuan, P.; Javey, A.; Malloy, R.; Wang, Q.; Bokor, J.; Dai, H., Monolithic integration of carbon nanotube devices with silicon MOS technology. *Nano Lett.* **2004**, *4*, 123-127. DOI: 10.1021/nl0349707

[5] Bianco, A.; Kostarelos, K.; Partidos, C. D.; Prato, M., Biomedical applications of functionalised carbon nanotubes. *Chem. Commun*. **2005**, *5*, 571-577. DOI: 10.1039/b410943k.

[6] Smart, S. K.; Cassady, A. I.; Lu, G. Q.; Martin, D. J., The biocompatibility of carbon nanotubes. *Carbon.* **2006**, *44*, 1034-1047. DOI: 10.1016/ j.carbon.2005.10.011.

[7] Shi Kam, N. W.; Jessop, T. C.; Wender, P. A.; Dai, H., Nanotube molecular transporters: internalization of carbon nanotube-protein conjugates into mammalian cells. *J. Am. Chem. Soc.* **2004**, *126*, 6850-6851. DOI: 10.1021/ja0486059

[8] Bianco, A., Carbon nanotubes for the delivery of therapeutic molecules. *Expert. Opin. Drug Deliv.* **2004**, *1*, 57-65. DOI: 10.1517/17425247.1.1.57.

[9] Foldvari, M.; Bagonluri, M., Carbon nanotubes as functional excipients for nanomedicines: II. Drug delivery and biocompatibility issues. *Nanomedicine: Nanotechnology, Biology and Medicine.* **2008**, *4*, 183-200. DOI: 10.1016/j.

[10] Agarwal, A.; Gupta, U.; Asthana, A.; Jain, N. K., Dextran conjugated dendritic nanoconstructs as potential vectors for anti-cancer agent. *Biomaterials.* **2009**, *30*, 3588-3596. DOI: 10.1016/j.

[11] Bhadra, D.; Bhadra, S.; Jain, S.; Jain, N. K., A PEGylated dendritic nanoparticulate carrier of fluorouracil. *Int. J. Pharm.* **2003**, *257*, 111-124. DOI 10.1016/S0378-5173(03)00132-7

[12] Kumar, P. V.; Asthana, A.; Dutta, T.; Jain, N. K., Intracellular macrophage uptake of rifampicin loaded mannosylated dendrimers. *J. Drug Target.* **2006**, *14*, 546-556. DOI:10.1080/10611860600825159

[13] Chauhan, A. S.; Sridevi, S.; Chalasani, K. B.; Jain, A. K.; Jain, S. K.; Jain, N. K.; Diwan, P. V., Dendrimer-mediated transdermal delivery: enhanced bioavailability of indomethacin. *J. Control. Release.* **2003**, *90*, 335-343. DOI: 10.1016/S0168-3659(03)00200-1.

[14] Esfand, R.; Tomalia, D. A., Poly (amidoamine)

(PAMAM) dendrimers: from biomimicry to drug delivery and biomedical applications. *Drug Discov. Today*. **2001**, *6*, 427-436. DOI: 10.1016/S1359-6446(01)01757-3.

[15] Tekade, R. K.; Kumar, P. V.; Jain, N. K., Dendrimers in oncology: an expanding horizon. *Chem. Rev.* **2008**, *109*, 49-87. DOI: 10.1021/cr068212n.

[16] Hampel, S.; Kunze, D.; Haase, D.; Krämer, K.; Rauschenbach, M.; Ritschel, M.; Büchner, B., Carbon nanotubes filled with a chemotherapeutic agent: a nanocarrier mediates inhibition of tumor cell growth. *Nanomedicine*. **2008**, *3*, 175-182. DOI: 10.2217/17435889.3.2.175

[17] Bianco, A.; Kostarelos, K.; Prato, M., Applications of carbon nanotubes in drug delivery. *Curr. Opin. Chem. Biol.* **2005**, *9*, 674-679. DOI: 10.1016/j.cbpa.2005.10.005.

[18] Feazell, R. P.; Nakayama-Ratchford, N.; Dai, H.; Lippard, S. J., Soluble single-walled carbon nanotubes as longboat delivery systems for platinum(IV) anticancer drug design. *J. Am. Chem.* **2007**, *129*, 8438-8439. DOI: 10.1021/ja073231f.

[19] Liu, Z.; Sun, X.; Nakayama-Ratchford, N.; Dai, H., Supramolecular chemistry on water-soluble carbon nanotubes for drug loading and delivery. *ACS Nano*. **2007**, *1*, 50-56. DOI: 10.1021/nn700040t.

[20] Hilder, T. A.; Hill, J. M., Modelling the encapsulation of the anticancer drug cisplatin into carbon nanotubes. *Nanotechnology*. **2007**, *18*, 275704. DOI: 10.1088/0957 4484/18/27/275704.

[21] Hilder, T. A.; Hill, J. M., Carbon nanotubes as drug delivery nanocapsules. *Appl. Phys.* **2008**, *8*, 258-26. DOI: 10.1016/j.cap.2007.10.011

[22] Pantarotto, D.; Singh, R.; McCarthy, D.; Erhardt, M.; Briand, J. P.; Prato, M.; Bianco, A., Functionalized carbon nanotubes for plasmid DNA gene delivery. *Angew Chem. Int. Edn. Engl.* **2004**, *116*, 5354-5358. DOI: 10.1002/anie.200460437.

[23] Re, G. D.; Peluso, A.; Minichino, C., Hydrogen bridges and electron transfer in biomolecules. Study of a possible mechanism on a model charge-recombination system. *Can. J. Chem.* **1985**, *63*, 1850-1856. DOI: 10.1139/v85-307.

[24] Peluso, A.; Brahimi, M.; Carotenuto, M.; Del Re, G., Proton-assisted electron transfer. *J. Phy. Chem A.* **1998**, *102*, 10333-10339. DOI: 10.1021/ jp981845o.

[25] Cukier R. I., Proton-coupled electron transfer through an asymmetric hydrogen-bonded interface. *J. Phys. Chem.* **1995**, *99*, 16101-16115. DOI: 10.1021/j100043a060.

[26] Cukier R. I.; Nocera D.G., Proton-coupled electron transfer. *Annu. Rev. Phys. Chem.* **1998**, *49*, 337-369. DOI: 10.1146/annurev.physchem.49.1.337.

[27] Stoner-Ma, D.; Jaye, A. A.; Ronayne, K. L.; Nappa, J., Meech, S. R.; Tonge, P. J., An alternate proton acceptor for excited-state proton transfer in green fluorescent protein: rewiring GFP. *J. Am. Chem. Soc.* **2008**, *130*, 1227-1235. DIO: 10.1021/ja0754507.

[28] Fiebig, T.; Chachisvilis, M.; Manger, M.; Zewail, A. H.; Douhal, A.; Garcia-Ochoa, I.; de La Hoz Ayuso, A. (1999). Femtosecond dynamics of double proton transfer in a model DNA base pair: 7-azaindole dimers in the condensed phase. *The J. Phys. Chem A, 103*, 7419-7431. DOI: 10.1021/jp991822p.

[29] Collman, J. P.; Hegedus, L. S.; Norton, J. R.; Finke, R. G., In., Principles and applications of organotransition metal chemistry; Univ Science Books. Mill Valley. 1987, CA, (Chapter 6).

[30] Heck, R. F.; Breslow, D. S., The reaction of cobalt hydrotetracarbonyl with olefins. *J. Am. Chem.* **1961**, *83*, 4023-4027. DOI: 10.1021/ja01480a017.

[31] Hegazi, M. F.; Borchardt, R. T.; Schowen, R. L., SN2-like transition for methyl transfer catalyzed by catechol-O-methyltransferase. *J. Am. Chem. Soc.* **1976**, *98*, 3048-3049. DOI: 10.1021/ja00426a079.

[32] Williams, I. H., Theoretical modeling of compression effects in enzymic methyl transfer. *J. Am. Chem. Soc.* **1984**, *106*, 7206-7212. DOI: 10.1021/ja00335a058.

[33] Cui, F. C.; Pan, X. L.; Liu, W.; Liu, J. Y., Elucidation of the methyl transfer mechanism catalyzed by chalcone O□methyltransferase: A density functional study. *J. Comput. Chem.* **2011**, *32*, 3068-3074. DOI: 10.1002/jcc.21890.

[34] Graham, I.; Refsum, H.; Rosenberg, I. H.; Ueland, P. M. (Eds.), Homocysteine metabolism: from basic science to clinical medicine. Springer Science & Business Media.2012 (Vol. 196).

[35] Georgieva, P.; Himo, F., Density functional theory

study of the reaction mechanism of the DNA repairing enzyme alkylguanine alkyltransferase. *Chem. Phys. Lett.* **2008**, *463*, 214-218. DOI: 10.1016/j.cplett.2008.08.043.

[36] Georgieva, P.; Wu, Q.; McLeish, M. J.; Himo, F., The reaction mechanism of phenylethanolamine N-methyltransferase: a density functional theory study. *Biochimica et Biophysica Acta (BBA)-Proteins and Proteomics*. **2009**, *1794*, 1831-1837. DOI: 10.1016/j.bbapap.2009.08.022.

[37] Cakici, O.; Sikorski, M.; Stepkowski, T.; Bujacz, G.; Jaskolski, M., Crystal structures of NodS N-methyltransferase from Bradyrhizobium japonicum in ligand-free form and as SAH complex. *J. Mol. Biol.* **2010**, *404*, 874-889. DOI: 10.2210/pdb3ofk/pdb.

[38] García, I. G.; Stevenson, C. E.; Usón, I.; Meyers, C. L. F.; Walsh, C. T.; Lawson, D. M., The crystal structure of the novobiocin biosynthetic enzyme NovP: the first representative structure for the TylF *O*-methyltransferase superfamily. *J. Mol. Biol.* **2010**, *395*, 390-407. DOI: 10.1016/j.jmb.2009.10.045

[39] Becke, A. D., Density–functional thermochemistry. III. The role of exact exchange. *The J. Chem. Phys.* **1993**, *98*, 5648-5652.DOI: 10.1063/1.464913.

[40] Larabi, R.; Abtouche, S.; Brahimi, M., Theoretical study of methyl group transfer assisted by proton transfer reaction in the N-acylated imidates. *J. Mol. Model.* **2014**, *20*, 1-9. DOI: 10.1007/s00894-014-2302-9.

[41] Dapprich, S.; Komáromi, I.; Byun, K. S.; Morokuma, K.; Frisch, M. J., A new ONIOM implementation in Gaussian98. Part I. The calculation of energies, gradients, vibrational frequencies and electric field derivatives. *J. Mol. Struct*., (THEOCHEM1). **1999**, *461*, 1-21. DOI: 10.1016/S0166-1280(98)00475-8.

[42] Frisch, M. G.; Trucks, G. W.; Schlegel, H. B.; Scuseria, G. E.; Robb, M. A.; Cheeseman, J. R.; Scalmani G.; Barone ,V.; Mennucci, B.; GA Petersson *et al*., Gaussian. Inc. Wallingford CT.2009.

[43] Jensen, F., Introduction to computational chemistry. West Sussex, England: John Wiley & Sons Ltd., 2007, 30-34.

[44] Svensson, M.; Humbel, S.; Froese, R. D.; Matsubara, T.; Sieber, S.; Morokuma, K., ONIOM: A multilayered integrated MO+MM method for geometry optimizations and single point energy predictions. A test for Diels-Alder reactions and Pt (P (t-Bu) 3) $2+H_2$ oxidative addition. *J. Phys. Chem.* **1996**, *100*, 19357-19363. DOI: 10.1021/jp962071j.

[45] Jansen, H. B.; Ros, P., Non-empirical molecular orbital calculations on the protonation of carbon monoxide. *Chem. Phys. Lett.* **1969**, *3*, 140-143. DOI: 10.1016/00092614(69)80118-1.

[46] Liu, B.; McLean, A. D., Accurate calculation of the attractive interaction of two ground state helium atoms. *J. Chem. Phys.* **1973**, *59*, 4557-4558. DOI: 10.1063/1.1680654

[47] Boys, S. F.; Bernardi, F. D., The calculation of small molecular interactions by the differences of separate total energies. Some procedures with reduced errors. *Mol. Phys.* **1970**, *19*, 553-566. DOI: 10.1080/00268977000101561.

[48] Rappé, A. K.; Casewit, C. J.; Colwell, K. S.; Goddard Iii, W. A.; Skiff, W. M., UFF, a full periodic table force field for molecular mechanics and molecular dynamics simulations. *J. Am. Chem. Soc.* **1992**, *114*, 10024-10035. DOI: 10.1021/ja00051a040.

[49] Ricca, A.; Drocco, J. A., Interaction of O_2 with a (9, 0) carbon nanotube. *Chem. Phys. Lett.* **2002**, *362*, 217-223. DOI: 10.1016/S0009-2614(02)01004-7.

[50] Liu, L. V.; Tian, W. Q.; Wang, Y. A., Chemical reaction of nitric oxides with the 5-1DB defect of the single-walled carbon nanotube. *J. Phys. Chem.* **2006**, *110*, 1999-2005. DOI: 10.1021/jp053931b.

[51] Rosi, M.; Bauschlicher, C. W., The functionalization of (5,5), (9,0), and (10,0) single wall carbon nanotubes by CH n fragments. *Chem. Phys. Lett.* **2007**, *437*, 99-103. DOI: 10.1016/j.cplett.2007.02.002

[52] Fu, A. P.; Li, H. L.; Du, D. M.; Zhou, Z. Y., Theoretical study on the reaction mechanism of proton transfer in formamide. *Chem. Phys. Lett.* **2003**, *382*, 332-337. DOI: 10.1016/j.cplett.2003.10.070.

[53] Wang, L.; Xu, J.; Yi, C.; Zou, H.; Xu, W., Theoretical study on the thermal decomposition of nitromethane encapsulated inside single-walled carbon nanotubes. *J. Mol. Struct., (THEOCHEM).* **2010**, *940*, 76-81. DOI: 10.1016/j.theochem.2009.10.013.

[54] Wang, L.; Yi, C.; Zou, H.; Xu, J.; Xu, W., On the

isomerization and dissociation of nitramide encapsulated inside an armchair (5,5) single-walled carbon nanotube. *Mater. Chem. Phys.* **2011**, *127*, 232-238. DOI: 10.1016/j.matchemphys.2011.01.065.

[55] Wang, L.; Yi, C.; Zou, H.; Gan, H.; Xu, J.; Xu, W., Initial reactions of methyl-nitramine confined inside armchair (5,5) single-walled carbon nanotube. *J. Mol. Model.* **2011**, *17*, 2751-2758. DOI: 10.1007/s00894-011-0967-x.

[56] Freitas, M. A.; O'Hair, R. A.; Williams, T. D., Gas Phase Reactions of Cysteine with Charged Electrophiles: Regioselectivities of the Dimethyl-chlorinium Ion and the Methoxymethyl Cation, 1. *J. Org. Chem.* **1997**, *62*, 6112-6120. DOI: 10.1021/jo9706741.

[57] Gunaydin, H.; Acevedo, O.; Jorgensen, W. L.; Houk, K. N., Computation of accurate activation barriers for methyl-transfer reactions of sulfonium and ammonium salts in aqueous solution. *J. Chem. Theory Comput.* **2007**, *3*, 1028-1035. DOI: 10.1021/ct050318n.